





Article

# Absolute Double-Differential Cross Sections of Ultrasoft Isochromatic X-ray Radiation in Electron Scattering on Atoms

Aleksei S. Kornev <sup>1</sup>, Boris A. Zon <sup>1</sup>, Vladislav E. Chernov <sup>1,\*</sup>, Miron Ya. Amusia <sup>2,†</sup>, Petr Kubelík <sup>3</sup> and Martin Ferus <sup>3</sup>

<sup>1</sup> Physics Faculty, Voronezh State University, 394018 Voronezh, Russia

<sup>2</sup> Racah Institute of Physics, The Hebrew University of Jerusalem, 91904 Jerusalem, Israel

<sup>3</sup> J. Heyrovský Institute of Physical Chemistry, Academy of Sciences of the Czech Republic, Dolejškova 3, 18223 Prague, Czech Republic

\* Correspondence: wladislav.chernov@gmail.com

† Also at: A. F. Ioffe Physical-Technical Institute, 194021 St. Petersburg, Russia

**Abstract:** We calculate double-differential cross sections of ultrasoft X-ray bremsstrahlung in electron scattering by Ar, Kr, and Xe atoms in the soft-photon approximation. The calculations are done for the isochromatic spectra (i.e., dependence on the electron energy at a fixed photon energy of 165 and 177 eV). The results are consistent with the absolute values of the differential cross sections measured by Gnatchenko et al. (Phys. Rev. A **80**, 022707 (2009)) for the above-mentioned photon energies. For low electron energies, our theoretical isochromatic spectra are in quantitative agreement with the experimental data for Ar. For Kr, the agreement is qualitative while agreement with the Xe data is poor.

**Keywords:** ultrasoft X-ray bremsstrahlung; isochromatic spectra



**Citation:** Kornev, A.S.; Zon, B.A.; Chernov, V.E.; Amusia, M.Y.; Ferus, M.; Kubelík, P. Absolute Double-Differential Cross Sections of Ultrasoft Isochromatic X-ray Radiation in Electron Scattering on Atoms. *Atoms* **2022**, *10*, 86. <https://doi.org/10.3390/atoms10030086>

Academic Editor: Anatoli Kheifets, Gleb Gribakin and Vadim Ivanov

Received: 11 August 2022

Accepted: 21 August 2022

Published: 24 August 2022

**Publisher's Note:** MDPI stays neutral with regard to jurisdictional claims in published maps and institutional affiliations.



**Copyright:** © 2022 by the authors. Licensee MDPI, Basel, Switzerland. This article is an open access article distributed under the terms and conditions of the Creative Commons Attribution (CC BY) license (<https://creativecommons.org/licenses/by/4.0/>).

## 1. Introduction

The long-wavelength range of the bremsstrahlung (BS) spectra has been studied for a long time because it is the region where the famous “infrared catastrophe” arises [1]. The relative intensity of BS in the long-wavelength range was first measured in [2] on thin metal targets bombarded by low-energy electrons. The experimental data were described well by the nonrelativistic Sommerfeld theory [3] which, in fact, is the theory of BS on a Coulomb center, accounting for the exponential screening of nuclei by the atomic electrons [4]. BS spectra play an important role in engineering and technical applications such as ion beam monitoring [5], plasma diagnostics [6], medical tomography imaging [7], etc.

In addition to the BS photon spectra, the dependence of BS cross sections on the scattering electron energy at a fixed photon energy (isochromatic spectra) is also of interest. These spectra were first measured for solid targets in [8], and the results are cited in a well-known monograph [9]. Korsunsky et al. [8] observed an increase of the BS probability from the zero value (at the minimal possible electron energy equal to the fixed photon energy) and a decrease of the BS probability at higher electron energy. A similar shape of the isochromatic spectra was registered for atomic targets in [10,11] in which the quasi-resonance character of the isochromatic spectra was observed. It should be noted that the detection technique for the isochromatic BS soft X-photons was proposed in [12,13]. A technique for detecting isochromatic BS photons in the UV range was proposed earlier in [14].

An analysis of the Sommerfeld [3] formula performed in [10] showed that an isochromatic spectrum maximum is achieved at the initial electron energy,  $E_i$ , equal to the following:

$$E_i^{\max} = 1.53 \hbar\omega, \quad (1)$$

where  $\omega$  is the photon frequency.

It should be noted that the knowledge of BS cross sections on atomic targets is important for studying BS generated in electron scattering on molecules [15] and clusters [16]. The “atomic” BS data are also used in Monte Carlo simulation of BS on solid targets (see, e.g., [17,18]).

All the above-cited works studied relative BS intensities only. At the same time, there exist some absolute BS cross-section value measurements. For example, high-precision ( $\approx 5.5\%$ ) absolute cross sections of BS on thin C, Al, Te, Ta, and Au targets have been recently measured in [19], which also contains references to earlier absolute BS cross-section measurements on solid targets.

To the authors’ best knowledge, the first absolute BS intensity measurements on atoms (Ne, Ar, Kr, and Xe) were performed in [20] for incident electron energies ranging from 28 to 50 keV. The experimental results were shown to be in qualitative agreement with the theory that takes into account not only the traditional BS mechanism (developed by Sommerfeld [3] for the nonrelativistic case and by Bethe and Heitler [21] and Sauter [22] for the relativistic case) but also the polarization bremsstrahlung (PBS) theory [23–25], which takes into account the photons emitted by the electrons of the atomic target. However, the quantitative difference between the experimental and theoretical results was quite significant, and this discrepancy increased with the decrease of BS photon energy. Similarly, discrepancy exists between the experimental cross sections measured in [19] and the data tabulated in [26,27], which also increases with the decrease of the BS photon energy. García-Alvarez et al. [19] noted this fact as one important result of their study. Similar discrepancy between theory and experiment was also observed in recent calculations [28].

However, the authors in [19,20] did not consider BS for photon energies in the ultrasoft X-ray region. Therefore, the absolute BS cross sections measured in [12,13] in the low-energy photon energy range are of great interest. These authors recorded the BS photon spectra for 600 eV electrons scattered on Ar, Kr, and Xe atoms, as well as the isochromatic spectra for the electron energies from 0.4 to 2 keV. Their results differ by 3–4 times from the calculations by Pratt et al. [29,30], who used the radial electron wavefunctions obtained in partial-wave series by numerically integrating the radial Dirac equation with a relativistic self-consistent screened potential. In recent calculations [28], the Dirac equation for the continuum wave function was solved by the power-series method with the interaction potential obtained from the Kohn–Sham density functional theory.

In the present work, we develop an interpretation of the experimental results of [12,13] using the soft-photon approximation (SPA); the validity conditions are discussed below. The general SPA formulas are presented in Section 2. SPA was used for interpretation of the ultrasoft X-ray spectra recorded in [31,32]. The BS photon spectra were measured in [12,13] for Ar, Kr, and Xe gaseous targets. Two types of BS spectra were recorded:

- (i) “Convenient” BS (or photon BS spectrum) that is the spectral and angular distribution of BS photons emitted in collisions with electrons whose energy,  $E_i$ , is fixed. Such spectra were analyzed in our recent study [33].
- (ii) Isochromatic BS spectrum that is the angular distribution of BS photons as function of the colliding electron energy,  $E_i$  (which varies in some interval), at a fixed photon energy,  $\hbar\omega$ . The isochromatic spectra are analyzed in Section 3 of the present work.

The results are discussed in Section 4. The main conclusions are given in Section 5.

## 2. Methods

### 2.1. General Formalism of Soft-Photon Approximation (SPA)

In the nonrelativistic SPA framework, the double-differential cross section,  $d\sigma_{\text{BS}}$ , of BS in the electron scattering on a target can be factorized. In particular,  $d\sigma_{\text{BS}}$  is the product

of the differential cross section,  $d\sigma_s$ , of the electron scattering on the same target without  $\gamma$ -radiation, by the probability,  $d\omega_\gamma$ , of the photon radiation [1]:

$$\begin{aligned} d\sigma_{BS} &= d\sigma_s d\omega_\gamma, \\ d\omega_\gamma &= \frac{\alpha}{4\pi^2} \left[ \frac{\mathbf{k}}{\omega} (\mathbf{v}_i - \mathbf{v}_f) \right]^2 \frac{d\omega}{\omega} d\Omega_\gamma. \end{aligned} \tag{2}$$

where  $\alpha \simeq 1/137$  is the fine structure constant,  $\mathbf{v}_i, \mathbf{v}_f$  are the electron velocity in the initial and final state, respectively;  $\mathbf{k}$  is the photon wave vector, and  $d\Omega_\gamma$  is the element of solid angle to which the photon is radiated. The cross section in (2) is averaged over the electron spin in the initial state and summed over the photon polarizations and the electron spin in the final state.

If the ejection direction of the electron is not fixed, we should integrate Equation (2) over this direction. To do this, we choose the  $z$  axis directed along the  $\mathbf{v}_i$  vector and write  $d\sigma_s$  in the following form:

$$d\sigma_s(E_i, \theta) = \sigma_s(E_i, \theta) d\Omega_{\mathbf{v}_f}, \tag{3}$$

where  $\theta$  is the polar angle of the  $\mathbf{v}_f$  vector,  $E_i$  is the energy of the impact electron. Then, Equation (2) can be written in the following form:

$$\begin{aligned} d\sigma_{BS} &= \frac{\alpha}{4\pi^2\omega} \sigma_s(E_i, \theta) \left[ \frac{v_i^2}{c^2} \cos^2 \Theta - \frac{2v_i}{c\omega} (\mathbf{k}\mathbf{v}_f) \cos \Theta \right. \\ &\quad \left. + \frac{(\mathbf{k}\mathbf{v}_f)^2}{\omega^2} \right] d\Omega_{\mathbf{v}_f} d\omega d\Omega_\gamma \\ &= \frac{\alpha}{4\pi^2 c^2 \omega} \sigma_s(E_i, \theta) \left[ v_i^2 \cos^2 \Theta \right. \\ &\quad \left. - 2v_i v_f \cos \Theta (\sin \Theta \sin \theta \cos \varphi + \cos \Theta \cos \theta) + \right. \\ &\quad \left. + v_f^2 (\sin \Theta \sin \theta \cos \varphi + \cos \Theta \cos \theta)^2 \right] d\Omega_{\mathbf{v}_f} d\omega d\Omega_\gamma. \end{aligned}$$

where  $\varphi$  is the azimuthal angle of the  $\mathbf{v}_f$  vector,  $\Theta$  is the polar angle of the  $\mathbf{k}$  vector (i.e., the angle between  $\mathbf{v}_i$  and  $\mathbf{k}$  vectors), and the azimuthal angle of the  $\mathbf{k}$  vector is assumed to be zero. After integration over  $\varphi$ , we obtain the following:

$$d\sigma_{BS} = \frac{\alpha}{2\pi c^2 \omega} \sigma_s(E_i, \theta) Q(\Theta, \theta) \sin \theta d\theta d\omega d\Omega_\gamma, \tag{4}$$

where

$$Q(\Theta, \theta) = v_i^2 \cos^2 \Theta - 2v_i v_f \cos^2 \Theta \cos \theta + v_f^2 \left( \frac{1}{2} \sin^2 \Theta \sin^2 \theta + \cos^2 \Theta \cos^2 \theta \right). \tag{5}$$

### 2.2. SPA: Validity Conditions

SPA is valid when the irradiated photon energy is low as compared to the scattering electron energy,  $E_i$ :

$$\omega \ll E_i/\hbar. \tag{6}$$

Apart the condition (6), it is also required for SPA validity that the momentum,  $\mathbf{q} = \mathbf{p}_i - \mathbf{p}_f$ , transferred to the atom from the scattering electron, is much higher than the electron momentum change due to irradiation of the photon [1]. In the nonrelativistic approximation, this condition takes the following form [1]:

$$\hbar\omega/(v_i q) \ll 1. \tag{7}$$

It is seen that the condition (7) is violated at low transferred momentum values, i.e., at small scattering angles,  $\theta$ . However, the contribution of the small angles into BS cross

section is small due to the angular factor,  $Q(\Theta, \theta)$  in Equation (4). This factor is plotted in Figure 1 as function of the scattering angle,  $\theta$ , for the value of  $\Theta = 83^\circ$  used experimentally in [12,13]. It is clearly seen that  $Q(\Theta, \theta)$  is small for  $\theta \rightarrow 0$ .

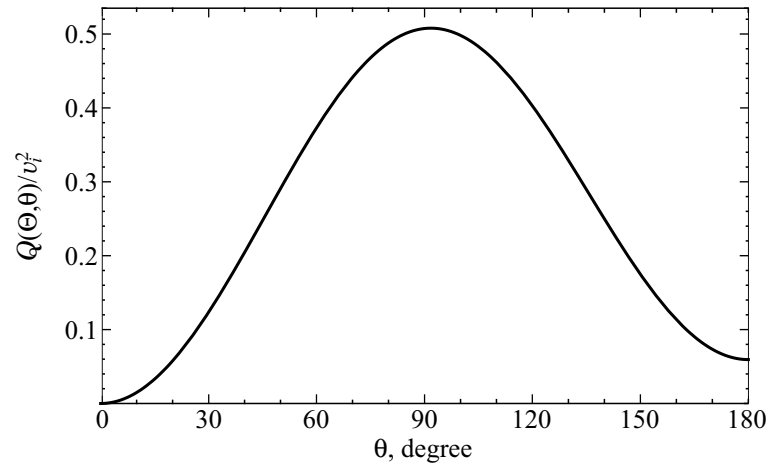


Figure 1. The angular factor,  $Q(\Theta, \theta)/v_f^2$ , from Equation (5) at  $\Theta = 83^\circ$  and  $v_f \simeq v_i$ .

### 3. Results on Isochromatic Spectra

Wavelength dependence of the BS intensity was obtained in experiment [13] and analyzed theoretically in [33].

Now, we proceed to the analysis of the isochromatic spectra. These spectra show the dependence of BS intensity on the electron energy,  $E_i$ , at a fixed photon energy,  $\hbar\omega$ . The authors in [13] list the experimental values for a modified (as compared to that in Equation (4)) differential BS cross section. This modification, as compared to Equation (4), implies calculating the angle-differential cross section of BS photon radiation into a finite small wavelength interval,  $\Delta\lambda$ , integrated over the scattering angle,  $\theta$ ,

$$\frac{d\sigma_{BS}}{d\Omega_\gamma} = \frac{\alpha}{2\pi c^2} \frac{\Delta\lambda}{\lambda} \int_0^\pi \sigma_s(E_i, \theta) Q(\Theta, \theta) \sin\theta \, d\theta, \tag{8}$$

where  $\lambda = 2\pi\hbar/k$  is the photon wavelength, the factor  $Q(\Theta, \theta)$  is defined in Equation (5). In other words, a change  $d\omega/\omega \rightarrow \Delta\lambda/\lambda$  should be done in Equation (4). In the experiment presented in [13], photons were registered in the wavelength interval of  $\Delta\lambda = 0.1$  nm. Equation (8) requires knowledge of the following integrals:

$$\mathcal{J}_{ab}(E_i) = \int_0^\pi \sigma_s(E_i, \theta) \cos^a \theta \sin^{1+b} \theta \, d\theta, \quad (ab) = (00), (10), (20), (02). \tag{9}$$

In particular, the cross section of elastic electron–atom scattering is  $\sigma_{el}(E_i) = 2\pi\mathcal{J}_{00}(E_i)$ .

Equation (8) implies using differential cross sections of elastic electron–atom scattering,  $\sigma_s(E_i, \theta)$ , tabulated as functions of the scattering angle,  $\theta$ . Such data can be obtained by numerical simulation using various models for interaction of the incident electrons with atoms. For instance, the cross-section database [34] contains data for the majority of atoms of the Periodic system. These data were used in our earlier work [33] for analysis of experimental BS photon spectra at fixed energy of an electron scattering on rare gas atoms [13].

In the case of electron scattering on argon atom, the data calculated in [35] can be used as an alternative to the NIST database [34]. The results of the cross-section calculation at particular electron energies,  $E_i$ , using both datasets are presented in Table 1.

**Table 1.** Simulated cross section in elastic electron–atom scattering ( $\text{\AA}^2$ ).

$E_i$ , keV	Ar			Kr		Xe	
	[34]	[35]	[36]	[34]	[36]	[34]	[36]
0.4	2.30	2.21	1.99	2.98	2.92	4.20	3.82
0.5	2.05	1.97	1.76	2.69	2.51	3.86	3.42
0.6	1.85	1.78	1.59	2.46	2.27	3.58	3.11
0.7	1.70	1.63	1.45	2.28	2.03	3.34	2.76
0.8	1.57	1.51	1.34	2.14	1.94	3.14	2.71
0.9	1.47	1.41	1.25	2.01	1.81	2.98	2.64
1.0	1.38	1.33	1.17	1.90	1.73	2.83	2.29
1.5	1.07	1.03	0.91	1.53	1.19	2.33	1.94
2.0	0.88	0.86	0.76	1.30	1.01	2.02	1.65

It can be seen that the cross sections of elastic electron scattering on Ar calculated in [34,35] coincide within 4%. However, the angle-differential cross sections differ significantly. As it is seen from Figure 2, the differential cross section has a sharp maximum for the forward scattering. This maximum calculated in [35] is two times higher as compared to the results of [34], and the differential cross section drops down for the scattering angles  $\theta > 15^\circ$ . Cross sections of electron scattering on Ar, Kr, and Xe atoms were also calculated in [36]. They are presented in Table 1 as well and their values are less as compared to those of [34]. This difference increases with the electron energy,  $E_i$ , up to 40% at  $E_i = 2$  keV. Unfortunately, the angle-differential cross sections are not listed in [36].

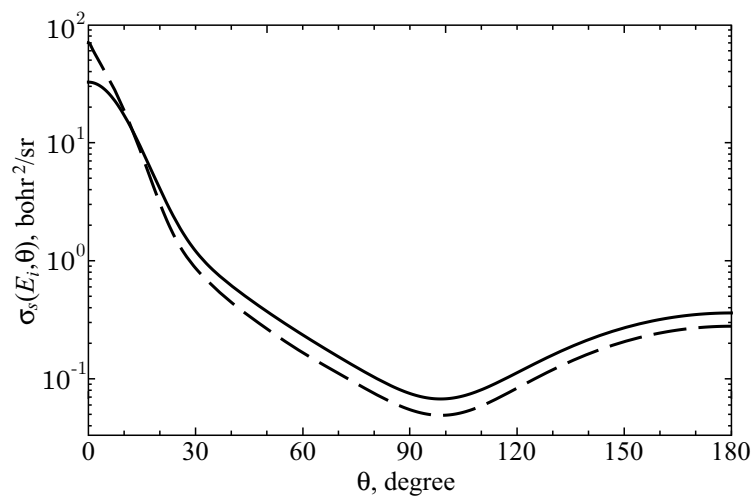


**Figure 2.** The differential cross section of elastic  $e$ –Ar scattering at  $E_i = 0.4$  keV from [34] (solid line) and from Figure 7a of [35] (dashed line).

The results of our calculations of isochromatic BS spectra by Equation (8) are given in Figures 3–5 in comparison with the experimental data shown in Figures 5–7 of [13], respectively. We note a misprint in [13]: the cross section shown in these figures should be measured in mbarn/sr, not barn. As seen from these figures, the calculated BS cross sections increase with the initial electron energy,  $E_i$ , for Kr and Xe, and slightly decrease for Ar. We recall that calculations of the isochromatic spectra according to Pratt et al. [29,30] (as given in [13]) predict a monotonic decrease of the BS intensity as a function of  $E_i$ .

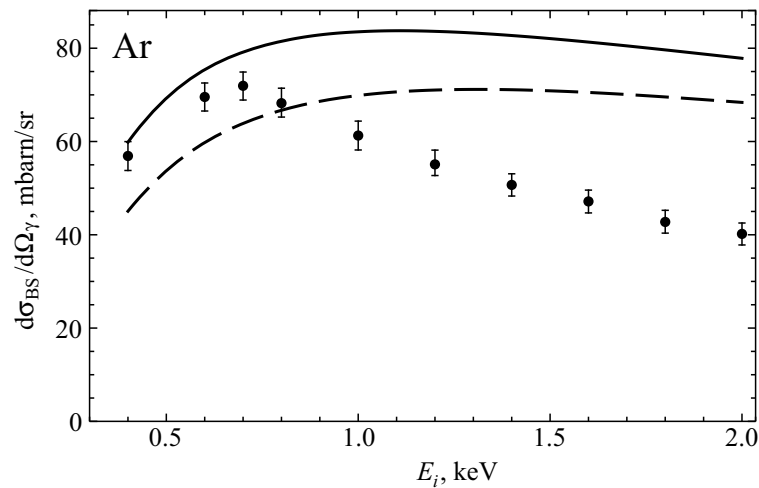


**Figure 3.** Isochromatic spectrum for Ar: double-differential BS cross section (8) as a function of the initial electron energy at the fixed photon energy of 177 eV. Solid line: elastic-scattering differential cross sections are taken from [34]; dashed line: from [35]. Black points with error bars: experimental values adopted from Figure 5 in [13] by manual digitization.

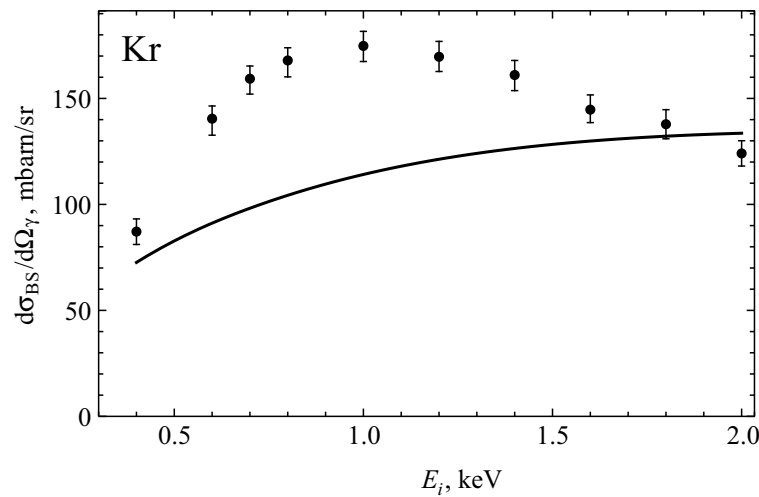


**Figure 4.** Same as in Figure 3 for Kr,  $\hbar\omega = 165$  eV. Experimental values adopted from Figure 6 in [13].

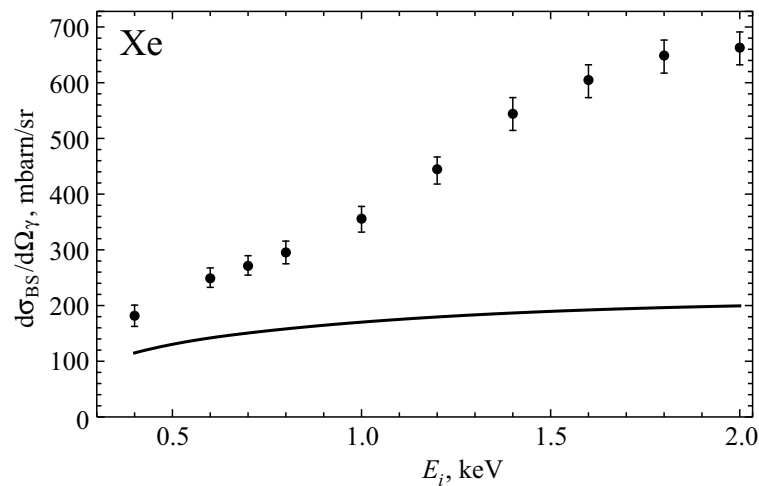


**Figure 5.** Same as in Figure 4 for Xe,  $\hbar\omega = 177$  eV. Experimental values adopted from Figure 7 in [13].

Note the maximum value of BS cross sections is reached at  $E_i = E_i^{\max}$  (see Equation (1)) and predicted by Sommerfeld [3] in the pure Coulomb potential. Under the conditions of the experiment of [13], this maximum should be observed at  $E_i \approx 0.26$  keV.

#### 4. Discussion

In the geometry of the experiment [13] ( $\Theta = 83^\circ$ ), according to Equation (5), the main contribution into the BS cross section (8) is made by the following term:

$$\left(\frac{d\sigma_{\text{BS}}}{d\Omega_\gamma}\right)_0 = \frac{\alpha}{4\pi c^2} \frac{\Delta\lambda}{\lambda} v_f^2 \sin^2 \Theta \mathcal{J}_{02}(E_i), \quad (10)$$

where the factor  $\mathcal{J}_{02}(E_i)$  is defined by Equation (9). The  $E_i$ -dependence in Equation (10) is due not only to the  $v_f^2$  factor but also to the  $\mathcal{J}_{02}(E_i)$  dependence.

For the total (scattering + impact ionization) cross section  $\sigma_{\text{tot}}(E_i)$ , this dependence on  $E_i$  in the range 0.5–2.0 keV, according to [36], can be approximated by the following equation:

$$\sigma_{\text{tot}}(E_i) \sim E_i^{-B}, \quad (11)$$

where parameter  $B$  varies from 0.90 for He to 0.59 for Xe. These values make the slow dependence (11) unable to compensate the linear increase of  $v_f^2$ . However, the dependence of  $\mathcal{J}_{02}$  on  $E_i$  can differ from (11). Of course, the discrepancy between theory and experiment can be also due to inaccuracy of SPA in this case.

In the case of argon (see Figure 3), the maximum in the isochromatic spectrum measured in [13] appears at the electron energy,  $E_i^{\text{expt}} = 0.7$  keV, which is greater compared to that given by Equation (1). For the energies less than 0.7 keV, our theoretical results are in satisfactory accord with the experiment. However, theoretical dependence of BS cross section on  $E_i$ , obtained using the differential cross section of elastic scattering from [34] has a less sharp maximum at  $E_i^{\text{theor}} = 1.11$  keV. When the differential cross-section data from [35] are used, the maximum appears at  $E_i^{\text{theor}} = 1.31$  keV. In both cases, the calculated cross section decreases with  $E_i$  slower compared to the experiment. Unfortunately, we have no explanation of such a behavior of the cross section. We note that using the elastic cross sections from [35] results in lesser BS cross section compared to using the data from [34] that make better agreement with the experiment. This can be caused by the fact that the results in [35] give (i) a more sharp maximum at the forward differential cross section and (ii) less magnitude of the cross section in the  $\theta > 15^\circ$  domain, as compared to [34] (see also Figure 2). It is this angular domain that makes the main contribution into the value of  $\mathcal{J}_{02}(E_i)$  in (9) due to  $\sin^3 \theta$  in the integral. Thus, in the case of Ar, we have quantitative agreement with the experiment at the electron energy  $E_i < E_i^{\text{expt}} = 0.7$  keV, and a qualitative agreement for higher energies.

In the case of krypton (see Figure 4), the experimental isochromatic spectrum [13] has the maximum at  $E_i^{\text{expt}} = 1.0$  keV which is higher than the value given by (1) as well. Our BS cross section calculated using the differential cross section of elastic scattering from [34], slowly increases in the studied energy range,  $E_i = 0.4$ –2.0 keV. Unfortunately, the authors in [35] do not provide differential cross sections of elastic  $e$ -Kr scattering, so our calculations for Kr can achieve only qualitative agreement with the experiment yet.

An even worse situation takes place for xenon (see Figure 5). Both experimental and theoretical isochromatic spectra increase with the electron energy,  $E_i$ , the former [13] increasing much faster than the latter. Extrapolating the Ar and Kr data, one can suppose that  $E_i^{\text{expt}}$  increases with the nuclear charge of the atomic target. Probably, one has  $E_i^{\text{expt}} > 2$  keV for Xe. A similar discrepancy between theoretical and experimental BS spectra in  $e$ -Xe scattering with fixed electron energy,  $E_i = 0.6$  keV, was noted in our earlier work [33]. A possible explanation of this discrepancy could be due to greater role of so-called polarization BS [23,31,37] for Xe, as compared to the lighter rare gases. Indeed, the main atomic

feature responsible for the polarization bremsstrahlung is the dipole polarizability [23]. The contribution of polarization BS into the experimental BS spectra of rare gases should increase with the nuclear charge since the polarizabilities of these gases are 11, 17 and 27 bohr<sup>3</sup> for Ar, Kr and Xe, respectively [38]. The discrepancy between theory and experiment for Kr isochromatic spectra can be also due to polarization BS, as well as to some inelastic processes, such as impact ionization (in Equations (4) and (8), we take into account conventional BS and elastic cross section only).

The main disadvantage of the presented theory is that it does not reproduce the BS intensity decrease for sufficient high electron energy,  $E_i > E_i^{\text{expt}}$ , as seen from Figure 4.

## 5. Conclusions

The isochromatic spectra recorded in [10] and studied in detail in [13] are quasi-resonant, i.e., demonstrate a prominent maxima at some electron energy  $E_i = E_i^{\text{expt}}$ . It should be noted that the experimental values of  $E_i^{\text{expt}}$  are much higher than those given by the BS theory,  $E_i^{\text{max}}$ , in pure Coulomb potential (1). This excess of  $E_i^{\text{expt}}$  value increases with the target nucleus charge. Therefore, the isochromatic spectra reported in [13] for Xe did not display any maxima, since the electron energies studied in [13] did not exceed 2 keV, which is probably lower than the  $E_i^{\text{max}}$  value for Xe. Our model gives the first quantitative description of the increase of BS intensity at low  $E_i < E_i^{\text{max}}$  in the isochromatic spectra for Ar and the first qualitative description for Kr and Xe. The other theoretical models [29,30] predict a monotonic (without maxima) decrease of the BS intensity as a function of  $E_i$ .

It should be emphasized that the agreement with experiment demonstrated in this work is achieved with the help of very simple analytical expressions.

Unlike the BS spectra with the fixed electron energy [13,33], the isochromatic spectra can possibly be more sensitive indicators of the polarization component of BS since this component appears not only in xenon, but probably also in krypton.

**Author Contributions:** Conceptualization, B.A.Z. and M.Y.A.; methodology, B.A.Z.; visualization, A.S.K. and V.E.C.; writing—original draft preparation, B.A.Z. and A.S.K.; writing—review and editing, M.Y.A. and V.E.C.; data curation, M.F.; software, P.K.; validation, A.S.K. and V.E.C.; formal analysis, A.S.K. and V.E.C.; funding acquisition, P.K. and V.E.C. All authors have read and agreed to the published version of the manuscript.

**Funding:** This research was funded by joint project of Czech Science Foundation (grant number 20-10591J) and Russian Foundation of Basic Research (grant number 19-52-26006) and Ministry of Science and Higher Education of the Russian Federation (grant number FZGU-2020-0035) and ERDF/ESF “Centre of Advanced Applied Sciences” (grant number CZ.02.1.01/0.0/0.0/16\_019/0000778).

**Institutional Review Board Statement:** Not applicable.

**Informed Consent Statement:** Not applicable.

**Data Availability Statement:** Not applicable.

**Acknowledgments:** The authors express their deep gratitude to A. A. Tkachenko for the detailed discussion of the experimental results presented in [12,13]. We are grateful to Prof. Fazlul Haque for kindly provided numerical data on cross section published in [35].

**Conflicts of Interest:** The authors declare no conflicts of interest.

## Abbreviations

The following abbreviations are used in this manuscript:

BS     Bremsstrahlung  
SPA    soft-photon approximation



## References

- Akhiezer, A.I.; Berestetskiĭ, V.B. *Quantum Electrodynamics; Interscience Monographs and Texts in Physics and Astronomy*; Interscience Publishers: New York, NY, USA, 1965; Volume 11.
- Peterson, T.J.; Tomboulion, D.H. Low-Energy Continuous X-Ray Spectrum in the 80 Å to 180 Å Region. *Phys. Rev.* **1962**, *125*, 235–241. [[CrossRef](#)]
- Sommerfeld, A. *Atombau und Spektrallinien*; Friedr. Vieweg und Sohn: Braunschweig, Germany, 1939; Volume 2.
- Kirkpatrick, P.; Wiedmann, L. Theoretical Continuous X-Ray Energy and Polarization. *Phys. Rev.* **1945**, *67*, 321–339. [[CrossRef](#)]
- Ralite, F.; Koumeir, C.; Guertin, A.; Haddad, F.; Mouchard, Q.; Servagent, N.; Métivier, V. Bremsstrahlung X-rays as a non-invasive tool for ion beam monitoring. *Nucl. Instrum. Methods Phys. Res. Sect. B* **2021**, *500–501*, 76–82. [[CrossRef](#)]
- Kwak, S.; Hergenhan, U.; Höfel, U.; Krychowiak, M.; Pavone, A.; Svensson, J.; Ford, O.; König, R.; Bozhenkov, S.; Fuchert, G.; et al. Bayesian inference of spatially resolved  $Z_{\text{eff}}$  profiles from line integrated bremsstrahlung spectra. *Rev. Sci. Instrum.* **2021**, *92*, 043505. [[CrossRef](#)]
- Talebi, A.S.; Rajabi, H. Outcomes following transarterial radioembolization with  $^{90}\text{Y}$  and nanoparticles loaded resin microspheres. *Appl. Radiat. Isot.* **2022**, *188*, 110405. [[CrossRef](#)]
- Korsunsky, M.I.; Walther, A.K.; Ivanov, A.V.; Zypkin, S.I.; Ganenko, V.E. An investigation of “Bremsstrahlung” by means of excited  $\text{In}^{115}$  nuclei. *J. Phys.* **1943**, *7*, 129–137.
- Massey, H.S.W.; Burhop, E.H.S.; Gilbody, H.B. *Electronic and Ionic Impact Phenomena. Vol. II. Electron Collisions with Molecules and Photo-Ionization*; Clarendon Press: Oxford, UK, 1969.
- Gnatchenko, E.V.; Tkachenko, A.A.; Verkhovtseva, E.T.; Zon, B.A. Ultrasoft X-Ray Bremsstrahlung Isochromatic Spectra from 300–2000 eV Electrons on Ar and Kr. *Phys. Rev. Lett.* **2005**, *95*, 023002. [[CrossRef](#)]
- Verkhovtseva, E.T.; Gnatchenko, E.V.; Tkachenko, A.A.; Zon, B.A. Resonance structures in polarization bremsstrahlung from electron–atom collisions. *Rad. Phys. Chem.* **2006**, *75*, 1115–1134. [[CrossRef](#)]
- Gnatchenko, E.V.; Tkachenko, A.A.; Nechay, A.N. Absolute differential bremsstrahlung cross section for the scattering of 0.6-keV electrons by xenon atoms. *JETP Lett.* **2007**, *86*, 292–296. [[CrossRef](#)]
- Gnatchenko, E.V.; Nechay, A.N.; Tkachenko, A.A. Absolute differential bremsstrahlung cross sections for 0.4–2-keV electrons scattered by Ar, Kr, and Xe atoms. *Phys. Rev. A* **2009**, *80*, 022707. [[CrossRef](#)]
- Prince, K.C. Detector for Bremsstrahlung-Isochromatic-Spectroscopy (BIS). U.S. Patent No. 4,871,915, 3 October 1989.
- Prajapati, S.; Singh, B.; Singh, B.; Shanker, R. Study of anisotropy of bremsstrahlung radiation emitted from 4.0 keV electrons in scattering by  $\text{CH}_4$  molecule. *Rad. Phys. Chem.* **2018**, *153*, 92–97. [[CrossRef](#)]
- Gnatchenko, E.V.; Nechay, A.N.; Samovarov, V.N.; Tkachenko, A.A. Polarization bremsstrahlung from xenon atoms and clusters: A cooperative effect contribution. *Phys. Rev. A* **2010**, *82*, 012702. [[CrossRef](#)]
- Li, L.; An, Z.; Zhu, J.; Tan, W.; Sun, Q.; Liu, M. Bremsstrahlung of 5–25-keV electron impact with Al, Cu, Ag, Te, and Au thick solid targets with no polarization contribution. *Phys. Rev. A* **2019**, *99*, 052701. [[CrossRef](#)]
- Li, L.; An, Z.; Zhu, J.; Liu, M. Experimental thick target bremsstrahlung spectra produced by 5–25 keV electrons for  $6 \leq Z \leq 82$  and comparison with Monte Carlo PENELOPE simulations. *Nucl. Instrum. Methods Phys. Res. Sect. B* **2019**, *445*, 13–17. [[CrossRef](#)]
- García-Alvarez, J.A.; Fernández-Varea, J.M.; Vanin, V.R.; Maidana, N.L. Electron-atom bremsstrahlung cross sections in the 20–100 keV energy region: Absolute measurements for  $6 \leq Z \leq 79$  and comparison with theoretical databases. *J. Phys. B At. Mol. Opt. Phys.* **2018**, *51*, 225003. [[CrossRef](#)]
- Portillo, S.; Quarles, C.A. Absolute Doubly Differential Cross Sections for Electron Bremsstrahlung from Rare Gas Atoms at 28 and 50 keV. *Phys. Rev. Lett.* **2003**, *91*, 173201. [[CrossRef](#)]
- Bethe, H.; Heitler, W. On the stopping of fast particles and on the creation of positive electrons. *Proc. R. Soc. London Ser. A* **1934**, *146*, 83–112. [[CrossRef](#)]
- Sauter, F. Über den atomaren Photoeffekt bei großer Härte der anregenden Strahlung. *Ann. Phys.* **1931**, *401*, 217–248. [[CrossRef](#)]
- Amus’ya, M.Y.; Biunistrov, V.M.; Zon, B.A.; Tsytoich, V.N.; Astapenko, V.A.; Kleiman, E.B.; Korol’, A.V.; Krotov, Y.A.; Kukushkin, A.B.; Lisitsa, V.S.; et al. *Polarization Bremsstrahlung; Physics of Atoms and Molecules*; Springer US: New York, NY, USA, 1992. [[CrossRef](#)]
- Astapenko, V. *Polarization Bremsstrahlung on Atoms, Plasmas, Nanostructures and Solids*; Springer Series on Atomic, Optical, and Plasma Physics; Springer: Berlin/Heidelberg, Germany, 2013; Volume 23. [[CrossRef](#)]
- Korol, A.V.; Solovyov, A.V. *Polarization Bremsstrahlung*; Springer Series on Atomic Optical and Plasma Physics (SSAOPP); Springer: New York, NY, USA, 2014; Volume 23. [[CrossRef](#)]
- Kissel, L.; Quarles, C.A.; Pratt, R.H. Shape functions for atomic-field bremsstrahlung from electrons of kinetic energy 1–500 keV on selected neutral atoms  $1 \leq Z \leq 92$ . *At. Data Nucl. Data Tables* **1983**, *28*, 381–460. [[CrossRef](#)]
- Seltzer, S.M.; Berger, M.J. Bremsstrahlung energy spectra from electrons with kinetic energy 1 keV–10 GeV incident on screened nuclei and orbital electrons of neutral atoms with  $Z = 1–100$ . *At. Data Nucl. Data Tables* **1986**, *35*, 345–418. [[CrossRef](#)]
- Poškus, A. Shape functions and singly differential cross sections of bremsstrahlung at electron energies from 10 eV to 3 MeV for  $Z = 1–100$ . *At. Data Nucl. Data Tables* **2019**, *129–130*, 101277. [[CrossRef](#)]
- Pratt, R.H.; Tseng, H.K.; Lee, C.M.; Kissel, L.; MacCallum, C.; Riley, M. Bremsstrahlung energy spectra from electrons of kinetic energy  $1 \text{ keV} \leq T_1 \leq 2000 \text{ keV}$  incident on neutral atoms  $2 \leq Z \leq 92$ . *At. Data Nucl. Data Tables* **1977**, *20*, 175–209. [[CrossRef](#)]

30. Pratt, R.H.; Tseng, H.K.; Lee, C.M.; Kissel, L.; MacCallum, C.; Riley, M. Bremsstrahlung energy spectra from electrons of kinetic energy  $1 \text{ keV} \leq T_1 \leq 2000 \text{ keV}$  incident on neutral atoms  $2 \leq Z \leq 92$ . *At. Data Nucl. Data Tables* **1981**, *26*, 477–481. [[CrossRef](#)]
31. Verkhovtseva, É.T.; Gnatchenko, E.V.; Zon, B.A.; Nekipelov, A.A.; Tkachenko, A.A. Bremsstrahlung in electron scattering by xenon. *Sov. Phys. JETP* **1990**, *71*, 443–448.
32. Zon, B.A. Bremsstrahlung in intermediate-energy electron scattering by noble gas atoms. *Sov. Phys. JETP* **1995**, *80*, 655–656.
33. Kornev, A.S.; Zon, B.A.; Amusia, M.Y. Absolute cross sections of ultra-soft x-ray radiation in electron scattering upon atoms and the soft-photons approximation. *Phys. Lett. A* **2019**, *383*, 2488–2491. [[CrossRef](#)]
34. Jablonski, A.; Salvat, F.; Powell, C.J.; Lee, A.Y. *NIST Electron Elastic-Scattering Cross-Section Database Version 4.0*; NIST Standard Reference Database Number 64; National Institute of Standards and Technology: Gaithersburg, MD, USA, 2016; p. 20899.
35. Haque, M.M.; Haque, A.K.F.; Jakubassa-Amundsen, D.H.; Patoary, M.A.R.; Basak, A.K.; Maaza, M.; Saha, B.C.; Uddin, M.A.  $e^\pm$  Ar scattering in the energy range  $1 \text{ eV} \leq E_i \leq 0.5 \text{ GeV}$ . *J. Phys. Commun.* **2019**, *3*, 045011. [[CrossRef](#)]
36. Vinodkumar, M.; Limbachiya, C.; Antony, B.; Joshipura, K.N. Calculations of elastic, ionization and total cross sections for inert gases upon electron impact: Threshold to 2 keV. *J. Phys. B At. Mol. Opt. Phys.* **2007**, *40*, 3259–3271. [[CrossRef](#)]
37. Amusia, M.Y.; Chernysheva, L.V.; Lee, T.J.; Almlöf, J. Bremsstrahlung spectrum on Xe for 600 eV electrons. *J. Phys. B: At. Mol. Opt. Phys.* **1990**, *23*, 2899. [[CrossRef](#)]
38. Rice, J.E.; Taylor, P.R.; Korol, A.V. The Determination of Accurate Dipole Polarizabilities  $\alpha$  and  $\gamma$  for the Noble Gases. *J. Chem. Phys.* **1991**, *94*, 4972. [[CrossRef](#)]